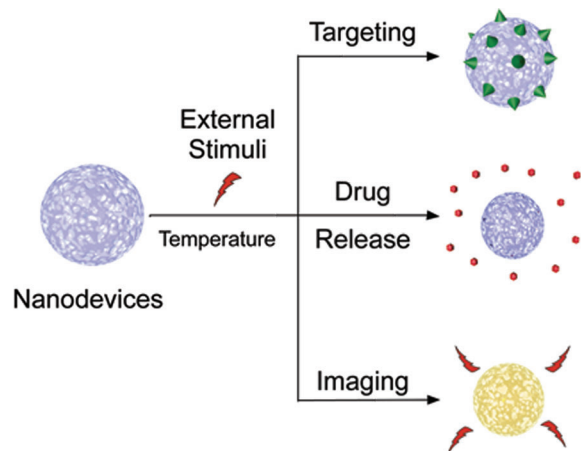


Thermoresponsive Nanodevices in Biomedical Applications

Julián Bergueiro, Marcelo Calderón*

In the last couple of decades several drug carriers have been tailored on the nanometric scale by taking advantage of new stimuli responsive materials. Thermoresponsive polymers in particular have been extensively employed as stimuli-responsive building blocks that in combination with other environmental-responsive materials allowed the birth of smarter systems that can respond to more than one stimulus. Examples that highlight the different polymers for thermally triggered drug delivery will be described. A special emphasis will be given to the description of novel theranostic nanodevices that combine more than one responsive modality in order to create a local hyperthermia that leads to the polymer phase transition and triggered drug release, cell recognition, and/or appearance of an imaging signal.



1. Introduction

The use of nanotechnology with different medical purposes had given birth to nanomedicine, one of the most promising research fields in the last decades.^[1] More precisely, nanomedicine applied to cancer therapies is one of the hot research topics nowadays. Materials in nanometric scale have several properties, which make them interesting for anticancer applications: (a) a defined 3D structure with a nanometric size that can take advantage of the cell internalization mechanisms or the enhanced permeability and retention (EPR)^[2] effect; (b) high drug loading capacity by means of drug encapsulation or conjugation; (c) different

switchable on/off properties that can be triggered by environmental signals; (d) tracking on the body by bioimaging techniques; and (e) specific recognition for selectively delivery to the site of action.^[3,4]

Biomedical nanosystems can be applied for therapy or diagnosis of cancer and other diseases. Common imaging materials for diagnosis make use of photoluminescence, mostly mediated by fluorescent groups, and magnetic resonance imaging through specific contrast agents. Common therapeutics approaches comprise drug delivery, gene delivery, photodynamic therapy, hyperthermia, and radiation therapy.^[5] The most advanced systems combine both therapy and diagnosis in approaches recently known as theranostics.^[6–8]

Materials that are able to sense and respond to environmental changes are known as smart.^[9] Of all the smart nanomaterials employed in disease treatments, thermoresponsive systems have shown high versatility due to the precise control of the response towards thermal changes. Usually the thermosensitivity of the system is achieved by the use of polymeric building blocks that

Dr. J. Bergueiro, Prof. M. Calderón
Institut für Chemie und Biochemie, Freie Universität Berlin
Takustrasse 3, 14195, Berlin, Germany
Fax: +49-30-838459368; E-mail: marcelo.calderon@fu-berlin.de
Prof. M. Calderón
Helmholtz Virtuelles Institut – Multifunctional Biomaterials for Medicine, Helmholtz-Zentrum Geesthacht, Teltow, Germany

respond to temperature. Such polymers have a sharp transition temperature at which their solubility in water dramatically changes. In this sense there are two main types of thermoresponsive polymers: The first presents a lower critical solution temperature (LCST) and the second presents an upper critical solution temperature (UCST). LCST and UCST represent respectively the critical lower and upper points in the temperature vs. polymer volume fraction ϕ phase diagram below and above which the polymer and solvent are completely miscible (Figure 1). Therefore an aqueous solution of a LCST polymer is clear and homogeneous below the transition temperature, because the polymer is perfectly soluble in water. But above the transition temperature the polymer becomes hydrophobic and water insoluble, whereupon the solution appears cloudy. The transition temperature at which this macroscopic effect takes place is also called cloud point (T_{CP}) and depends on the concentration of the polymer as well as the concentration of other components in the system like salts, etc.^[10] UCST polymers, on the other hand, are water soluble above the T_{CP} and hydrophobic below this temperature because of the known hydrophobic effect.^[11] Mostly polymers that have a LCST have been employed in research. It is worth to mention that some block polymers could have more than one transitions due to a micellation of the system.^[12] Figure 2 presents some of the monomers that have been utilized for their synthesis.

2. Building Blocks

Thermoresponsive polymers with T_{CP} near the body temperature of around 37 °C are especially interesting for biomedical applications.^[13,14] Poly(*N*-isopropylacrylamide) (PNIPAm) is the most extensively studied thermoresponsive polymer because of its LCST in water of around 32 °C. It is commonly prepared by radical polymerization of



Prof. Marcelo Calderón is an Assistant Professor for Macromolecular and Organic Chemistry at the Department of Biology, Chemistry, and Pharmacy from the Freie Universität Berlin, Germany. Dr. Calderón received his Ph.D. in organic chemistry in 2007 from the National University of Córdoba, Argentina, under the supervision of Prof. Miriam Strumia. In 2007 he joined the Research Group of Prof. Rainer Haag at the Freie Universität Berlin for his Postdoctoral work, where he pursued the development of polymer-drug conjugates for the passive targeted delivery of drugs, genes, and imaging probes. Dr. Calderón was the recipient of the Arthur K. Doolittle Award in 2010 (American Chemical Society, Polymer Materials: Science and Engineering Division), the Cesar Milstein Fellowship in 2011 (Ministry of Science, Technology and Productive Innovation, Argentina), and the Nano-MatFutur Grant for Young Scientists from the German Ministry of Science in 2012 (BMBF).



Dr. Julián Bergueiro received his BS and MS in Chemistry from the University of Santiago de Compostela (Spain) in 2007 and 2008, respectively. In 2013 he received his PhD from USC under the supervision of Prof. S. Lopez. In 2012 he joined the group of Prof. R. Riguera to work on the synthesis and characterization of stimuli-response helical polymers and poly(phenylacetylene)s@gold nanoparticles nanocomposites. He joined Prof. M. Calderón group in 2013 to carry out his postdoctoral research at Freie Universität Berlin. Recently he was awarded with a Dahlem International Network Postdocs Fellowship to develop gold based thermoresponsive nanogels as nanocarriers.

the monomer *N*-isopropylacrylamide (NIPAm). Its phase transition temperature can be conveniently adjusted by copolymerization with other acrylic monomers. If hydrophilic monomers like acrylic acid (AA) are incorporated randomly into the polymer, the phase transition temperature is increased as well as the electrostatic absorption of positively charged drugs such as doxorubicin-HCl (Dox).

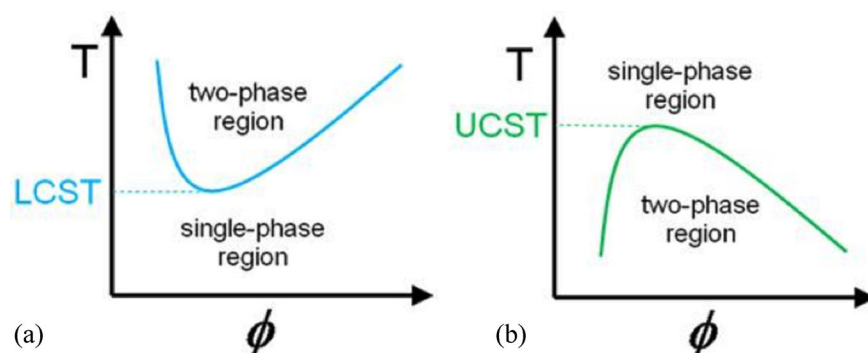


Figure 1. Temperature vs. polymer volume fraction, ϕ . Schematic illustration of phase diagrams for polymer solution with (a) lower critical solution temperature (LCST) behavior or (b) upper critical solution temperature (UCST) behavior. Reproduced with permission.^[10] Creative Commons 2011, MDPI.

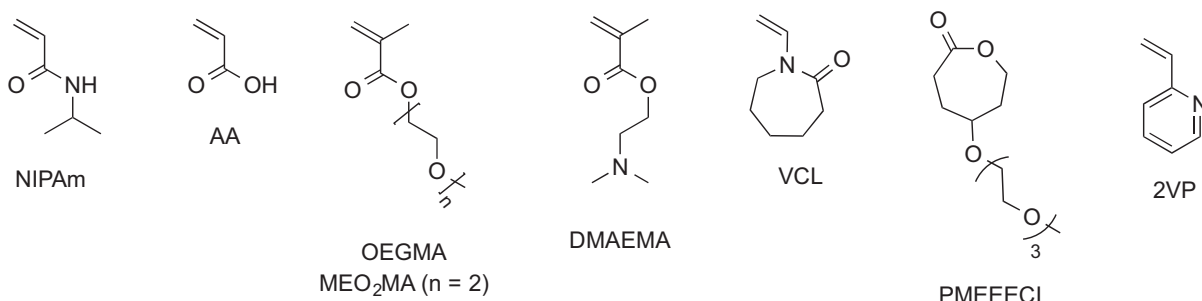


Figure 2. Commonly used precursor monomers for the synthesis of thermoresponsive polymers.

Conversely, when a hydrophobic monomer is used, the transition temperature is decreased.^[10]

Poly(oligoethylene glycol) methacrylates (POEGMA) are another type of intensively studied thermoresponsive polymers because of their neutral, nontoxic, and non-immunogenic character.^[15] Moreover, their T_{CP} can be tuned by the size of the OEG segment and also by copolymerization with 2-(2-methoxyethoxy) ethyl methacrylate (MEO₂MA).^[16] Tertiary amine-containing methacrylates based polymers like poly[2-(dimethylamino)ethyl methacrylate] (PDMAEMA) have shown a dual-responsive behavior in aqueous solution where the cloud point is dependant on the pH value.^[17,18] PDMAEMA based polycations demonstrated good gene transfection properties that have been used to transport nucleic acids into cells.^[19]

Poly(*N*-vinylcaprolactam) (PVCL) is a known biocompatible polymer used for pharmaceutical purposes and derived from an inexpensive commercially available monomer, *N*-vinyl caprolactam (VCL).^[20–22] Unlike PNIPAm, it exhibits a classical Flory–Huggins thermoresponsive phase behavior in water (Type I). This means its LCST value decreases with the increasing polymer chain length and/or concentration. Therefore, its T_{CP} can be adjusted by controlling the polymer molecular weight without a co-monomer requirement.^[23] γ -Substituted caprolactone monomers can be polymerized in a ring opening fashion to generate new polymers like poly{g-[2-(2-methoxyethoxy)ethoxy-3-caprolactone]} (PMEEECL) with a LCST of about 48 °C.^[24]

One of the most commonly employed UCST polymers in drug delivery is poly(2-vinylpyridine) (P2VP) in its protonated form (P2VPH⁺). When combined with LCST polymers in a block structure, amphiphiles with useful temperature control can be achieved.^[25] At a temperature under the LCST or over the UCST, the block copolymer behaves as an amphiphile but remains perfectly soluble between the two transition temperatures (UCST < T < LCST). This conduct is very interesting for the construction of nanosystems.

Recently, reports showed the thermoresponsive behavior in disulfide bond based redox-responsive LCST polymers.

Higher T_{CP} values were obtained for the reduced entities in comparison with the T_{CP} of the polymers containing disulfides. This interesting ability can be applied to activate temperature dependant delivery systems in redox cellular environment.^[26,27]

Free radical polymerization (FRP) is a methodology commonly used for the synthesis of thermoresponsive polymers from vinyl-bearing monomers (PNIPAm, PVCL, PDMAEMA, POEGMA, or P2VP). However, FRP has inherent termination and transfer reactions that limit the control over the molecular weight distribution of the polymeric material. LCST molecular weight non-dependent thermoresponsive polymers like PNIPAm are usually synthesized with FRP since the weight distribution is not affecting the T_{CP} , but this presents a huge drawback to achieve a sharp and controlled transition temperature in molecular weight dependent polymers like PVCL, POEGMA, etc. It is known that mixtures of polymers like POEGMA of different sizes or high weight distribution give broader transitions in comparison with the well defined ones.^[28,29]

The so-called living radical polymerization (LRP) or controlled radical polymerization (CRP) techniques emerged several years ago to overcome this drawback.^[30] These radical polymerizations have a living like character and no termination or chain transference steps. Certainly, LRP have many of the desirable features of a FRP, like compatibility with a wide range of monomers, tolerance of functional groups, and simple reaction conditions. In addition, LRP enable a precise control of the polymer architecture (random, block) as well as the molecular weight, molecular weight distribution, and additional site-specific functionality. Among the existing LRP techniques, reversible addition-fragmentation chain transfer (RAFT)^[31] and atom transfer radical polymerization (ATRP)^[32] are the most widely used in the synthesis of thermoresponsive polymers since they are versatile processes and tolerant to a wide variety of reaction conditions and functionalities.

Some polymers like poly(ϵ -caprolactone) (PCL), poly(ethylene glycol) (PEG), or polylactide (PLA) are commonly synthesized by anionic ring opening polymerization

(AROP), which is described as a nucleophilic attack of the growing chain end on a heterocyclic monomer molecule.^[33] Ring opening metathesis polymerization (ROMP) has been used to synthesize norbornene based OEG. In a ROMP a cyclic olefin is converted into linear polymers containing olefins in the main chain, which releases in the polymerization the ring strain in the cyclic olefin monomer. A transition metal catalyst, i.e., Ruthenium (Ru), Molybdenum (Mo), Titanium (Ti), Tungsten (W), is needed in these kinds of polymerizations, for which the Grubbs catalyst is the most employed.^[33]

Elastin-based polypeptides (ELP) have recently attracted attention because of their high biocompatibility, temperature sensitivity, cellular recognition sequences, and uniformity in terms of particle size and size distribution. ELPs are repetitions of a basic unit pentapeptide sequence, e.g. glycine-valine-glycine-valine-proline (GVGVP), derived from the elastomeric domain of mammalian tropoelastin. These peptides have a thermoresponsive behavior in water and their phase transition can be dually triggered by temperature or pH. ELPs were used in drug delivery systems as block co-polymers forming micellar structures that retain their temperature sensitivity. ELPs can be obtained by chemical synthesis with the aid of peptide coupling techniques or by recombinant DNA technology involving gene construction, *Escherichia coli* transformation, and expression. Advantages of recombinant DNA technology are the precise control of not only the sequence and stereochemistry of amino acids but also the molecular weight and its distribution.^[34–38]

Hydroxybutyl chitosan (HBC) is a novel LCST thermosensitive polymer synthesized by modification of the free hydroxyls of chitosan to hydroxybutyl groups. Chitosan is an attractive and easy material for obtaining biopolymer since it is produced by alkaline N-deacetylation of chitin that is found in the exoskeletons of shellfish and crustaceans. HBC has shown to have excellent biocompatibility and minimal cytotoxicity.^[39] HBC has been widely utilized in medicine related areas like tissue engineering,^[40] post-operative treatment,^[39] and therapeutics delivery.^[41]

Hairpin-DNAs (hp-DNA) are DNA aptamers with a close-loop hairpin like conformation. The hydrogen bonds between the bases in the close-loop section can be broken to open the hairpin structure. A rise in the temperature facilitates this quasi “DNA melting” process, which makes these aptamers thermoresponsive ligands. These DNA molecules have been applied as temperature sensors on a nanometric scale, for example like temperature switches and thermometers or environment sensors. High sensitivity can be obtained in specifically desired temperature ranges.^[42] The synthesis of hp-DNA can be easily done by amplifying predefined DNA sequences by polymerase chain reaction (PCR).^[43]

Some of the smart nanosystems presented here are not only composed of thermoresponsive units, but also of other building blocks that have a structural function and contribute to the smartness of the system acting as triggers or labels. Polymeric dendrons which have desirable properties as a drug carrier can be used as soft building blocks like dendritic poly(amidoamine) dPAMAm or dendritic polyglycerol (dPG).^[49] Another soft material employed is graphene which can act as transducer of near infrared (NIR) radiation into heat.^[44] More precisely, photothermal transducers in the NIR frequency are of special interest for biomedical applications since the NIR radiation has a minimal absorbance by skin and tissues. NIR light can penetrate up to 10 cm deep, depending on the light power.^[45–47]

Hard nanoparticles constitute another type of building block with interesting properties commonly used in the construction of smart nanodevices for medical applications. They can act as therapeutic, diagnosis, or even theranostic agents. Gold nanoparticles (AuNPs) are the most used ones, particularly gold nanorods (AuNRs) with their surface plasmonic resonance in the NIR frequency can act as efficient photothermal transducers.^[48] Iron magnetic nanoparticles (MNPs) or magnetic nanobeads (MNBs) show photothermal transducer behavior under an alternating magnetic field and can also be easily functionalized.^[49–51] Quantum dots (QDs) and Gadolinium (Gd) complexes are widely used for imaging purposes and are of great interest.^[52,53]

The rational combination of the materials described above have already demonstrated the huge potential of thermoresponsive polymers for the emerging field of theranostics. The great amount of research activity currently being performed in this area of nanomaterials is increasing the number of available building blocks and improving the existing ones. Thus the number of reported smart nanodevices that combine these interesting properties has grown as well. This feature article resumes the state of the art in the field of thermoresponsive nanodevices for drug delivery, from the last 4 to 5 years, with a special focus on research that has relevance for the design and applicability of polymeric systems. The selected nanodevices have been classified by architectural complexity and polymer type.

3. Thermoresponsive Nanosystems

Different nanometric devices based on thermoresponsive colloids have been applied to overcome known problems in drug delivery. In the following, we review a selection of these devices which have been classified by their system's architecture.

3.1. Polymeric Micelles

Polymeric micelles (PMs) are self-assembled core-shell like structures formed by amphiphilic block copolymers. Micelles are generated when the concentration of amphiphiles in aqueous solutions increases above the critical micelle concentration (CMC).^[54,55] Typically these systems are not covalently cross-linked, being the micelle stabilization caused by the hydrophobic interaction between the hydrophilic blocks or by electrostatic interactions in the case of charged macromolecules. The most studied block copolymers in micellation are AB and ABA type copolymers. The thermoresponsive block is usually the hydrophilic part, in the case of LCST polymers, that is located on the outer side of the micelle. Once the T_{CP} of the thermoresponsive polymer has been reached, the hydrophilic stabilization disappears, which induces the disassembly of the micelle. Such mechanisms have great potential as a drug delivery system for the transport and thermally triggered release of compounds that are hydrophobic and have poor bioavailability like the anticancer drug Dox.^[56] The typical methods used for encapsulation of poorly water soluble drugs are dialysis, solid dispersion, complexation, chemical conjugation, and solvent evaporation procedures.^[57]

Most of the reported carriers make use of PNIPAm as thermoresponsive polymer (Table 1). A simple approximation was made by the Kanazawa group growing PNIPAm by RAFT polymerization and activating the terminal carboxyl group of the chain-transfer agent (mercaptopropionic acid) with *N*-hydroxysuccinimide for subsequent coupling to 5-aminofluorescein (FL) which acts as the

hydrophobic part. LCST of the system with or without FL did not suffer much alteration, 32.0 and 32.8 °C respectively. Copolymerizations with hydrophilic comonomers like butyl methacrylate (BMA) or hydrophobic ones like *N,N*-dimethylaminopropylacrylamide (DAMAAm) were performed to control the transition temperature. The LCST decreased until 27.7 °C with 3% of BMA, but rose until 37.4 °C with 2% of DAMAAm. Internalization studies in macrophage-like cells RAW 264.7 were performed that showed a precise temperature-dependent internalization of the fluorescent probe into the cells.^[58]

Another study of the cellular uptake mechanism of thermoresponsive polymeric micelles was reported by Nakayama and Okano. Block copolymers of hydrophilic PNIPAm and hydrophobic poly(D,L-lactide) (PLA) were the basis of this study in which the LCST was tuned by the copolymerization of NIPAm and *N,N*-dimethylacrylamide (DMAAm) in the RAFT polymerization. Maleimide (Mal) or its derivative Oregon Green 488 (OG) were conjugated to the RAFT agent, and tetramethylrhodamine (TAMRA) was linked to the terminal hydroxyl groups of PLA. These three block copolymers showed to have LCST values of 39.5, 39.2, and 40 °C, respectively. When visualized by a confocal laser scanning microscope, the internalization in bovine carotid endothelial cells was significantly limited below the micellar LCST but was greater at temperatures above it, most probably due to the enhanced interactions with the cell membrane. Micelles were internalized by the endocytosis mechanism and localized in the Golgi apparatus and endoplasmic reticulum, which made them good candidates for cell organelle targeting approaches.^[59] Micelles formed of

Table 1. Summary of the micellar systems discussed.

Thermoresponsive Polymer	Copolymer/Modification	Polymerization Type	Transition Temperature [°C]	Theranostic Agent	Ref.
PNIPAm	BMA/DAMAAm	RAFT	32.0–37.4	FL	[58]
P(IPAAm-DMAAm)	PLA	RAFT/ROP	39.5/40.0	TAMRA/Maleimide	[59]
P(NIPAm-co-DMAc)	PLA/PCL	RAFT/ROP	39/40.5	Dox	[60]
PNIPAm	L-histidine	RAFT/ROP	34.2–37.2	Dox	[61]
c-PNIPAm	PCL	ROP	25/30	Dox	[62]
P(NIPAm-co-NBA)	POEGMA	RAFT	5	Gd/Dox	[63]
PNOEG	NCA	ROMP	52.7/68.4	PTX	[64]
PMEECL	PMECL	ROP	31.1–48.6	_ ^{b)}	[65]
Chitosan	Deoxycholic acid	_ ^{a)}	38.2	Dox	[66]
ELP	SLP _{BC}	Recombinant	34	NGR tripeptide	[67]
ELP	ELP ₆₀	Recombinant	33–41	RGD	[68]

^{a)}Commercial sources; ^{b)}not reported.

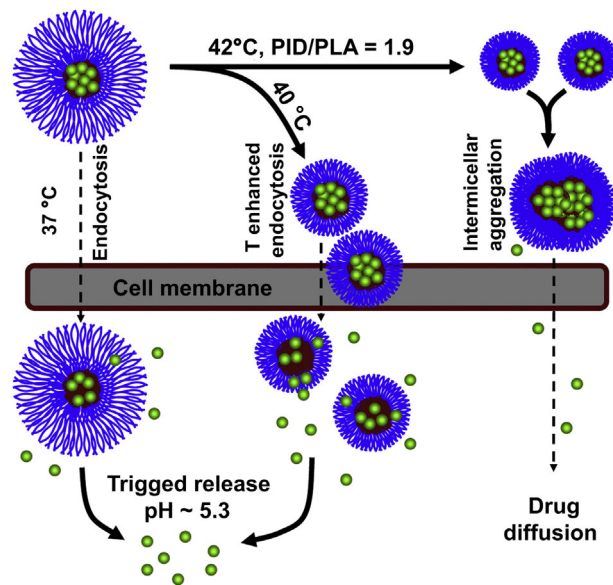


Figure 3. Illustration of the temperature regulated intracellular uptake P(NIPAm-c-DMAAm)-b-PLA (PID/PLA) micelles and the drug release process. Reproduced with permission.^[60] Copyright 2011, Elsevier.

block copolymers of PLA or PCL and PNIPAm-*co*- DMAAm not only had thermoresponsive behavior with a LCST of 40 °C of the shell but also pH-mediated degradation of the micelle core (Figure 3). It was observed that the intracellular uptake was 4 times greater at a temperature above the micellar phase transition. Dox was encapsulated and released *in vitro* in N-87 cancer cells at different temperatures, but it was found that the intermicellar aggregation due to temperature bounced back in cytotoxicity assays. This interesting example demonstrated that the internalization and drug release could be triggered by a combination of increased thermal triggers and acidic intracellular environment.^[60]

Another dual stimuli response micellar system, designed for delivering Dox into liver carcinoma, was reported by Kim et al.^[61] The micelles were formed by a block copolymer of PNIPAm as the thermoresponsive and hydrophilic block and ROP polymerized poly(*L*-histidine) as the pH-responsive and hydrophobic section. The number of units of the hydrophobic part was varied to control the LCST of the system. The higher number of units yielded higher T_{CP} values: for $X = 50, 75, 100, 125$ in $[p(\text{NIPAm})_{55}-b-p(\text{His})_X]$ the LCST were 34.2, 36.7, 36.3, and 37.5 °C, respectively. These systems also showed a pH dependant behavior, with micelles forming in aqueous solutions at pH values ranging from 6 to 10 and aggregates at a more acid pH. Release of Dox was evaluated by dialysis method at 37 °C at different pH values and showed good drug load efficiency values (36–51%). The drug loading content and

efficiency were higher in systems composed of more histidine units. The positive antitumor effect of the pH and temperature dependant release of Dox was demonstrated *in vitro* with HepG2 human hepatocellular carcinoma cell lines, which indicates the potential of these systems for drug delivery.

A cyclic form of PNIPAm was prepared by Liu et al. in the design of tadpole-shaped amphiphilic based micelles. Cyclic hydrophilic units of c-PNIPAm were easily synthesized by linear ATRP polymerization and ring closure by click chemistry with an alkyl-alcohol functionalized moiety. PCL was grown as a hydrophobic chain by ROP starting on the hydroxyl functionality of the c-PNIPAm. After self-assembly, the LCST of the micellar coronas was in the range 25–30 °C (Figure 4). Drug loading (26.3% encapsulation efficiency) took place upon micellation of these amphiphiles and the release was slightly higher at temperatures above the LCST. (c-PNIPAm)-*b*-PCL micelles showed marginal cytotoxicity up to a concentration of 1 mg · mL⁻¹ while Dox loaded micelles caused 60% of Hela cell death at the same concentration.^[62]

The same research group reported another micellar core-shell system in which the hydrophobic part of the amphiphile was the thermoresponsive polymer poly-

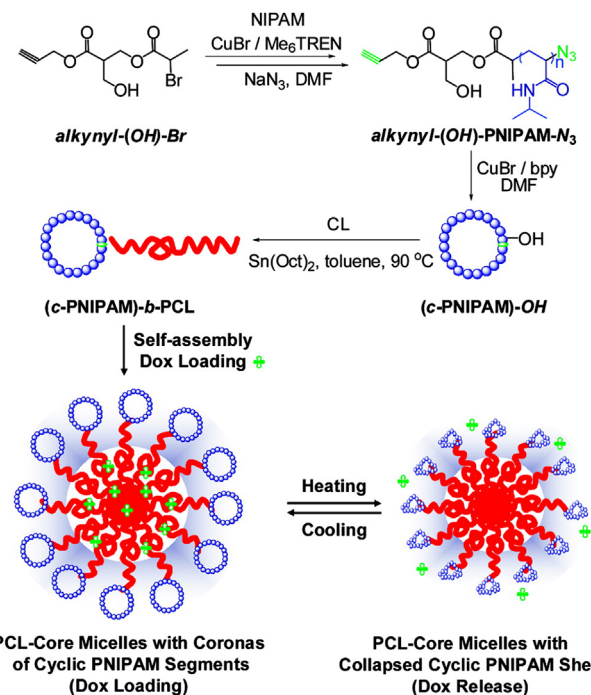


Figure 4. Synthesis of well-defined amphiphilic and thermoresponsive tadpole-shaped linear-cyclic diblock copolymer, (c-PNIPAM)-*b*-PCL, and its self-assembly in aqueous solution into micellar nanoparticles consisting of PCL cores and coronas of cyclic PNIPAM segments exhibiting thermo-induced collapse and aggregation behavior. Reproduced with permission.^[62] Copyright 2011, American Chemical Society.

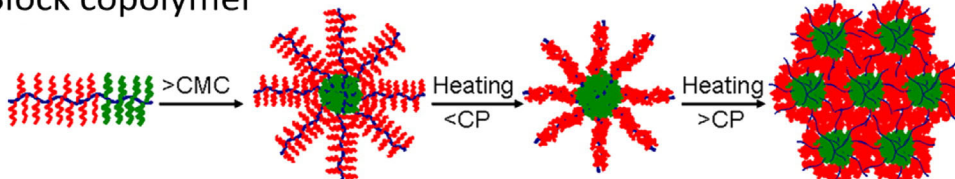
(NIPAm-*co*-2-nitrobenzyl acrylate) [P(NIPAm-*co*-NBA)] and the hydrophilic one was based on POEGMA. The polymer amphiphiles were synthesized by RAFT block copolymerization of OEGMA, NIPAm, NBA, and glycidyl methacrylate (GMA). The block copolymer was functionalized with an azide group in the GMA monomer for further attachment by click chemistry to the alkynyl-DOTA-Gd moiety (DOTA is 1,4,7,10-tetraaza-cyclododecane-1,4,7,10-tetrakis(steic acid)). The copolymers were designed to have a LCST of 5 °C and the thermosensitive block was therefore hydrophobic at room temperature, behaving like an amphiphile, and being able to encapsulate Dox. UV irradiation on the micellar dispersion triggered the cleavage of the NBA moiety which changed the hydrophobicity of the overall system and raised the LCST of the copolymer over 37 °C. This caused the hydrophobic-hydrophilic transition of the micellar cores to take place, which was associated with a core swelling and Dox release. The Gd complex masked in the hydrophobic phase was turned on as well as a magnetic resonance contrast agent. The system was tested with Hep2 cells and while 88% of them survived without UV irradiation, only 48% survived after 30 min of light radiation.^[63]

With the aim towards analyzing the micellar aggregation behavior of structurally diverse amphiphilic copolymers, Zhu et al. copolymerized norbornene derivatives bearing OEG as a hydrophilic monomer and cholic acid (CA) as the hydrophobic monomer using ROMP. As shown in Figure 5, both were synthesized as block and random copolymers. PNOEG-*b*-PNCA and P(NOEG-*r*-NCA) had a similar cloud point of around 60 °C. Micelles formed by the block copolymers exhibited a gradual shrinkage when heated

up to temperatures below the T_{CP} . Contrary, micelles formed with the random copolymer, however, exhibited micelle swelling in the same temperature range. Both types of micelles aggregated at temperatures above the T_{CP} . Both micelles were tested as nanocarriers with paclitaxel (PTX) in SKOV-3 cells and had good values in the cytotoxicity assays, although the random copolymer showed a closer to linear release profiles which is desirable in a drug delivery system.^[64]

Thermoresponsive micellar systems based on less common LCST polymers were also designed. As an example, di-block copolymers based on γ -substituted caprolactone like poly[γ -(2-methoxy)- ϵ -caprolactone]-block-poly{ γ -2-[2-(2-methoxyethoxy) ethoxy- ϵ -caprolactone} [P-MECL-*b*-MEECL] have been explored as potential drug delivery systems. In these copolymers, PMECL is the hydrophobic block and PMEEECL the hydrophilic and thermoresponsive part. These biodegradable polymers had tunable transition temperatures in the range of 31–43 °C by changing the monomers composition.^[65] Chen recently reported the fine tuning of the hydrophobic/hydrophilic balance in deoxycholic acid decorated hydroxybutyl chitosan polymers (DAHBC) by tailoring chitosan with hydrophilic hydroxybutyl groups (HB) and hydrophobic deoxycholic acid (DA) moieties. LCST values were adjusted by changing the mass ratios of DA and HB to an optimal value for hyperthermia therapy of 38.2 °C. Using Dox as a model drug, the chitosan based nanoparticles were tested as nanocarriers for in vitro delivery in MCF-7 cell line and shown to have an enhanced cytotoxicity in temperatures over the LCST.^[66]

Block copolymer



Random copolymer

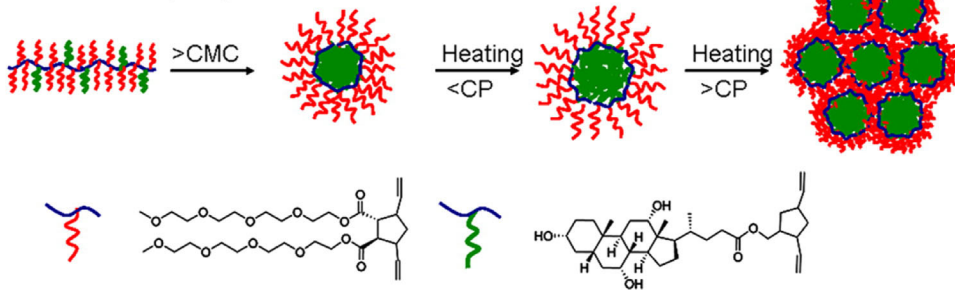


Figure 5. Schematic illustration of self-assembly and phase transition of block and random copolymers in water. Reproduced with permission.^[64] Copyright 2014, American Chemical Society.

One of the newest micellar delivery systems nowadays is based on ELPs. These genetically engineered amphiphilic block copolymers were designed to have cloud temperatures between 33 and 41 °C. ELP block copolymers were hydrophilic unimers that self-assembled into monodisperse spherical micelles with a nanometric diameter above the critical micellar temperature (CMT) through selective desolvation and collapse of the hydrophobic block. Upon increase of the temperature above the CMT, the micelles were stable until a second transition temperature was reached, which led to micelle aggregation. The transition temperature could be regulated by the size of each of the blocks. Chiltoki et al. decorated ELPs with targeting peptides like asparagyl-glycyl-arginine (NGR)^[67] that targeted the enzyme membrane CD13 associated with angiogenic tumor vessels and arginyl-glycyl-aspartic acid (RGD)^[68] peptide with $\alpha_V\beta_3$ integrin as receptor. Interestingly, both decorated ELPs demonstrated active tumor targeting in vivo only at temperatures about their CMT.

3.2. Polymersomes

Amphiphilic block copolymers can also self-assemble into vesicular architectures, which are called polymersomes. The dimensions, morphology, and properties of these structures can be controlled by varying the chemical constitution and size of the copolymer, the preparation methods (mainly solvent free and solvent displacement), and the solution properties (polymer concentration, pH, temperature, and solvent). Due to their hollowed morphology these structures can encapsulate different agents within the hydrophilic hollow or the hydrophobic bilayer. This makes polymersomes perfect candidates as nanocarriers for theranostics agents with different chemical properties (Table 2).^[69] Feijen et al. designed polymersomes formed by the biodegradable block copolymer m-PEG-co-P_{DLLA} containing a PNIPAm solution inside the hollow space at 25 °C. Above the LCST of PNIPAm (32 °C) phase separation took place, triggering the release of the therapeutic agents encapsulated within. Fluorescein-isothiocyanate (FITC)-labeled dextran was used as a model and

exhibited a faster release in the polymersomes containing PNIPAm at a temperature of 37 °C.^[70]

As shown in Figure 6, PEG₄₅-*b*-PtNEA_n copolymers were prepared to use the thermoresponsivity of a block copolymer to control the polymersome formation and therefore the drug encapsulation and release. PEG₄₅-*b*-PtNEA_n of different sizes ($n = 22, 44, 63, 91, 172$) were prepared by ATRP of *trans*-N-(2-ethoxy-1,3-dioxan-5-yl) acrylamide (tNEA) as a thermosensitive monomer and PEG as an hydrophilic macroinitiator. Vesicles were stable at physiological pH but the ortho esters of PtNEA became hydrolyzed under mildly acidic conditions. This caused the subsequent increase in hydrophilicity of the thermo-responsive block that triggered the dissociation of the polymersomes. This mechanism was found to be useful for the release of Dox and FITC-labeled lysozyme (FITC-lys) which were loaded in the hydrophobic part of the polymersomes and in the inner cavity, respectively. Dox loaded micelles showed a concentration dependent cytotoxicity towards tumor cells (HepG2). Therefore these particles may have a great importance as nanocarriers in the fields of intracellular drug delivery and/or combinational therapeutics.^[71]

Pluronic F127® is the commercial name for a ABA triblock copolymer of poly(ethylene oxide) (PEO) (hydrophilic) and poly(oxypropylene) (PPO) (hydrophobic) that was reported to form vesicle like empty core structures.^[72] Pluronic F127® was employed as thermoresponsive nanocapsules for drug delivery after decoration with chitosan by peptide coupling yielding copolymers with T_{CP} of around 25–30 °C. Ethidium bromide (EB) was encapsulated at 4 °C as a proof of concept and was released in a controlled manner at 37 °C after drying, dialysis, and cold shock treatment. In vitro assays with cancerous (MCF-7) and non-cancerous (C3H10T1/2) cells lines revealed a high specificity of the copolymers for the cancerous lines.^[73]

3.3. Core-shell Nanodevices

Core-shell composite nanoparticles are a unique class of materials that have been widely studied as delivery

Table 2. Summary of the polymersome systems discussed.

Thermoresponsive Polymer	Copolymer/Modification	Polymerization Type	Transition Temperature [°C]	Theranostic Agent	Ref.
PNIPAM	PEG-P _{DLLA}	ATRP/ROP	32	FITC-Dextran	[70]
PtNEA	PEG	ATRP	14–23	Dox-FITC-Lys	[71]
PEO/PPO	Chitosan	_ ^{a)}	25–30	EB	[73]

^{a)}Commercial sources.

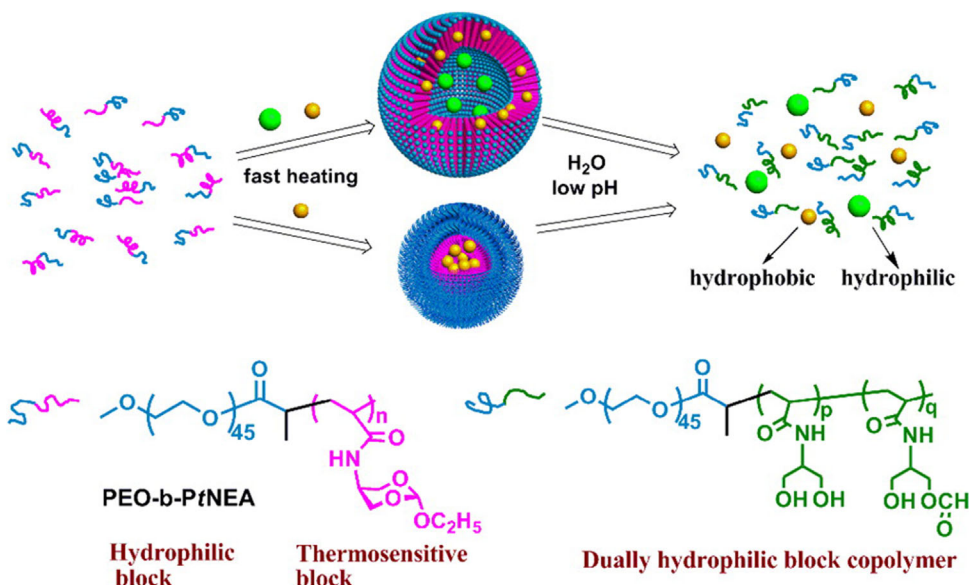


Figure 6. Thermally induced formation and acid-triggered dissociation of spherical nanoparticles and polymersomes. Reproduced with permission.^[7] Copyright 2013, American Chemical Society.

vehicles. They can be synthesized by surface reaction, seed growing polymerization, or layer-by-layer self-assembly, among other methodologies. In the case of core-shell thermoresponsive nanodevices, the thermoresponsive polymer is generally located on the surface. The core can be formed either by a hard nanoparticle or a soft material like a dendritic polymer or highly cross-linked polymers (nanogels).^[74]

3.3.1. Soft Materials Based Core-Shell Nanodevices

Several types of polymers, as summarized in Table 3, have been used as soft materials for the construction of core-shell systems. Dendritic polymers have raised the most attention due to their multifunctional character.^[9] PAMAm is one of the most intensively investigated dendrimers for many biomedical and pharmaceutical

areas. PAMAm dendrimers are highly desirable for the design of carriers for acidic drugs since their interiors exhibit high affinity for molecules with negative charge. For this reason, Wang et al. attached PNIPAm and PEG linear polymers to PAMAm dendrimers to obtain two kinds of nanostructures with different cloud points. The LCST of PNIPAm (32°C) was not modified upon coupling to PAMAm to yield the PAMAm-*g*-PNIPAm copolymer. The LCST rose to 35°C , however, when the hydrophilic/hydrophobic balance was changed upon the coupling to PEG (PAMAm-*g*-PNIPAm-*c*-PEG). The nanoparticles were loaded with indomethacin as the drug model, revealing a temperature-triggered drug release. At the biological temperature of 37°C , the thermoresponsive shell which was in hydrophobic phase kept the drug loaded in the core and only achieved a release of less than 30%. At a temperature below the LCST, i.e., 30°C , the PNIPAm became

Table 3. Summary of the soft-core-shell systems discussed.

Thermoresponsive Polymer	Core	Polymerization Type	Transition Temperature [$^{\circ}\text{C}$]	Theranostic Agent	Ref.
PNIPAm	PAMAm	ATRP/ROP	32/35	Indomethacin	[75]
P(NIPAm- <i>c</i> -AAm)	H40-PCL	ROP/ATRP	39.5	PTX	[76]
P(NIPAm- <i>c</i> -AAm)	RNGO@SiO ₂	ATRP	41	Dox	[77]
PNIPAm	P2VPH ⁺ /SO ³⁻	FRP	20–55	2,6-NDS	[78]
PNVCL	Chitosan	FRP	37	5-FU	[79]
ELP	PAMAm	Peptide coupling	48	RB	[80]

soluble and the system was therefore able to release the drug up to 80% within a period of 10 h.^[75]

The inverse thermoresponsive drug release behavior was reported with dendritic polyesters like Boltorn® H40 which had been grafted by ATRP with the block copolymers of PCL and P(NIPAm-*c*-AAm). This core-shell system was surface decorated with PEG, the fluorophore FL, and folate as the targeting moiety via copper-mediated click chemistry. The transition temperature of the nanoparticles was 39.5 °C, and the PTX release of these particles was enhanced at temperatures above the LCST, as it was shown by in vitro studies. The release at slightly acidic pH conditions was also higher than at physiological pH. Uptake of these nanocarriers in HeLa cells was increased because of the folate receptor mediated endocytosis.^[76]

P(NIPAm-*c*-AAm) was used to functionalize mesoporous silica shell coated reduced graphene oxide nanosheets (rNGO). The core-shell nanostructures formed by this method were engineered for controlled chemo-photothermal synergistic cancer therapy that was remotely controlled by IR radiation. As shown in Figure 7, rNGO

generated a local hyperthermia upon NIR irradiation that caused the hydrophobic transition of the thermoresponsive polymer and the subsequent release of an encapsulated drug. Interestingly, the Dox encapsulated within the core-shell system did not show any considerable cytotoxic effects against HeLa cells, if NIR laser irradiation was not applied. Almost the same percentage of killed cells was obtained upon NIR exposition as with free Dox. This recent example represents one of the state of the art approaches as far as thermoresponsive light triggered systems are concerned.^[77]

Yin and Liu recently reported an innovative combination of LCST and UCST polymers for the design of pH and temperature dual responsive systems (Figure 8). The nanoparticle core was based on the UCST polymer P2VPH⁺ slightly cross-linked with the counterion SO₃²⁻. The polymer PNIPAm was utilized as outer shell and LCST component. The nanosystems formed with this configuration showed transition temperatures (UCST and LCST) in a range of 20–55 °C. The hydrophilic fluorescent derivative sodium 2,6-naphthalenedisulfonate (2,6-NDS) was encapsulated in the core via electrostatic interactions with P2VPH⁺ and

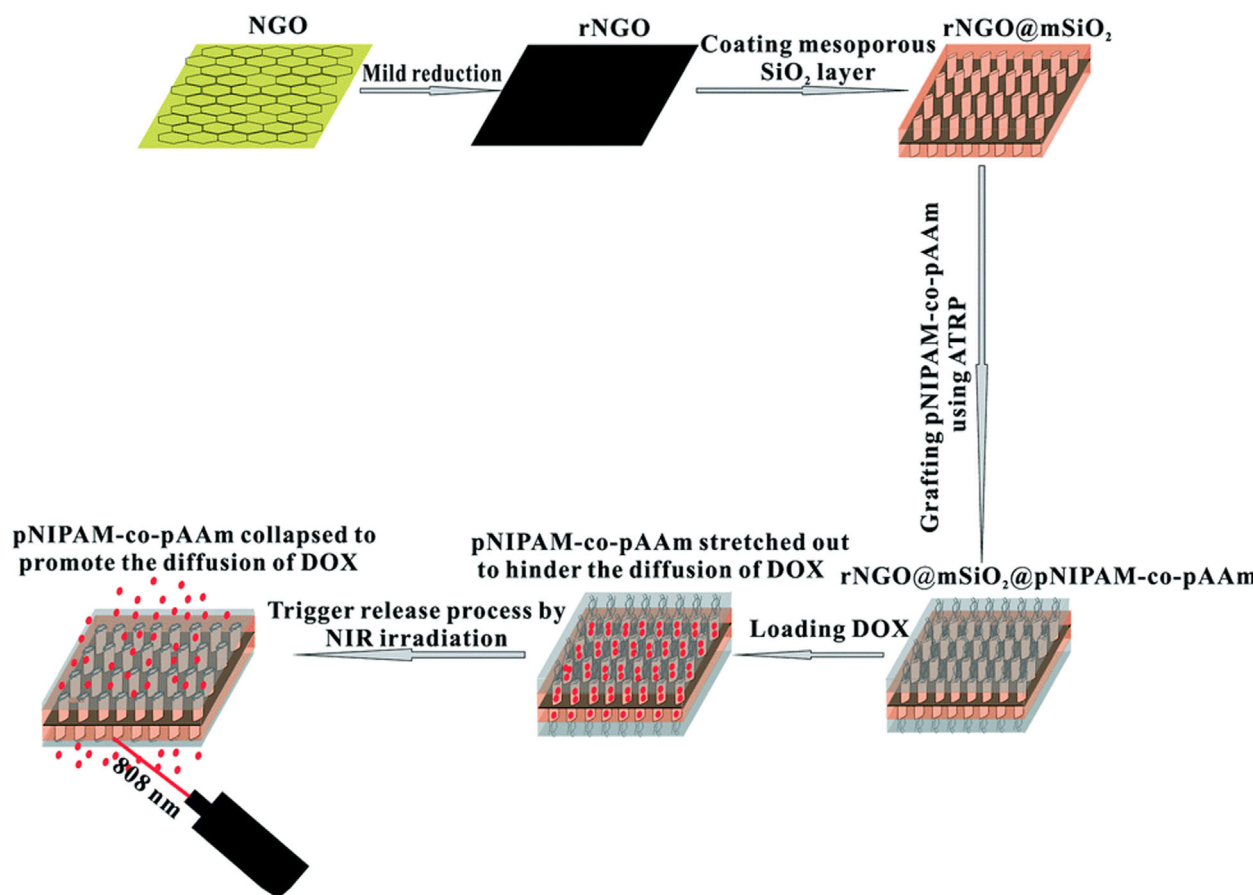


Figure 7. Fabrication process of rNGO@mSiO₂@PNIPAM-*c*-PAAm and Dox delivery mediated by NIR laser irradiation. Reproduced with permission.^[77] Copyright 2014, Royal Society of Chemistry.

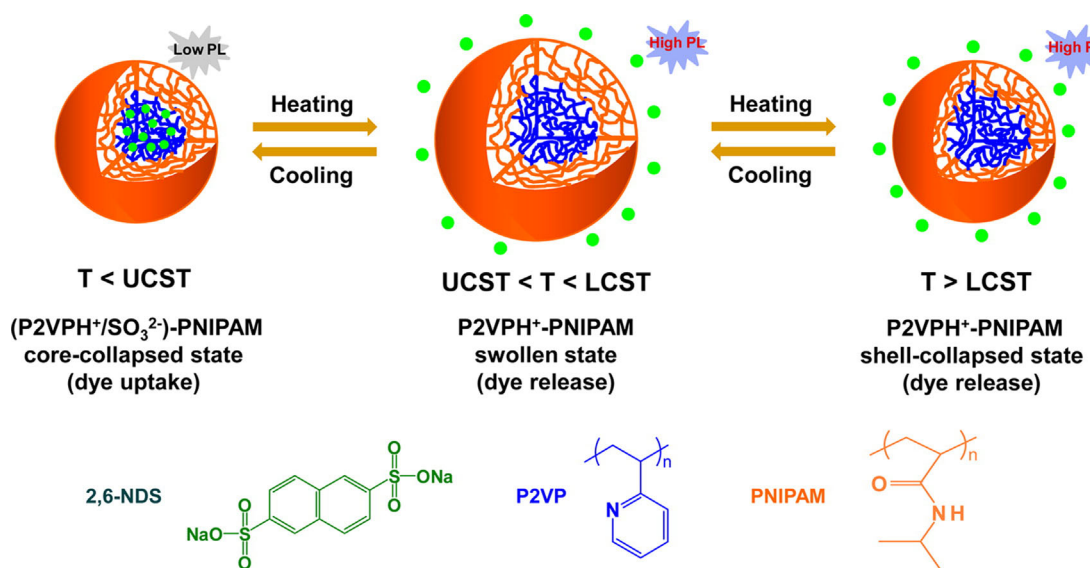


Figure 8. Schematic illustration of the reversible thermoresponsive volume phase transition of P2VP-PNIPAm core – shell copolymer at low pH as well as its thermo-induced uptake and release of 2,6-NDS in aqueous dispersion. Reproduced with permission.^[78] Copyright 2014, American Chemical Society.

its controlled release was monitored by fluorescence spectra. At temperatures above the UCST, 2,6-NDS was released from the core, highlighting the potential of these novel nanoparticles as perfect vehicles for highly hydrophilic drugs.^[78]

Chitosan was also used as the core of drug nanocarrier particles grafted with a shell of cross-linked thermoresponsive PNVCL. The authors proposed that the cross-linked shell helped to retain the drug after encapsulation. The LCST achieved of 38 °C was convenient for the biological applications of these nanocarriers and was tested with drugs like 5-fluorouracil (5-FU) as model. These nanodevices were specifically designed to overcome limitations of the free drug by increasing its circulation time and efficacy *in vivo*. Release experiments demonstrated that 5-FU was almost not released from the nanocarrier below the LCST, but upon heating over the transition point, the achieved release was more than 40%. Internalization of the nanoparticles was confirmed with rhodamine-123 labeled particles in PC3 cell lines. Cytotoxicity revealed an effective drug release in PC3 (prostate cancer), KB (oral cancer), and MCF7 (breast cancer) cell lines. The results were also confirmed by fluorescence-activated cell sorting (FACS) based apoptosis assay on mouse fibroblast cell line L929 and MCF7.^[79]

PAMAm fourth-generation dendrimers were used as the scaffold for the synthesis of ELP mimetic with the sequence Ac-Val-Pro-Gly-Val-Gly by peptide coupling chemistry. The resulting core-shell nanoparticles presented pH and NaCl concentration-dependant LCST, with a transition temperature at pH = 7 and 0.15 M NaCl of 48 °C.

As observed by circular dichroism, the elastin-mimetic dendrimer formed a β-turn structure upon heating. Rose Bengal (RB) was exploited in encapsulation and release assays to test the potential of this elastin-mimetics as drug carriers. The release profile of RB was similar to the pristine dendrimer, nevertheless this novel system is currently under investigation.^[80]

3.3.2. Hard Nanoparticles Based Core-Shell Nanodevices

Due to their defined architectures, well-established ligation mechanisms, photo-optical, luminescent, heating, and/or magnetic properties, hard nanoparticles based on different metals have been widely used in the construction of biomedical nanodevices (Table 4).^[81–83] The facile ligand exchange and the photo-optical properties make gold nanostructures the most used hard nanoparticles in this field. RAFT agents with trithioester groups have proven to be suitable linkers for binding RAFT synthesized polymers to AuNPs. Monteiro and Toth studied this ligation with AuNPs of different sizes (5, 10, and 20 nm) and different RAFT linear polymers, including thermoresponsive PNIPAM. AuNP@PNIPAM core–shell systems presented a LCST of 32 °C and a strongly thermal dependency of the size that increased from 15–20 to 110–590 nm when the temperature rose over the LCST. The uptake of the particles in Caco-2 cells at 37 °C increased from approximately 2% after 30 min to 8% after 2 h, values much greater than the negative or neutral AuNPs. This is believed to be result of hydrophobic interactions between the core–shell system and the cell membrane.^[84] AuNP@P(NIPAm-*c*-Am)

Table 4. Summary of the hard-core-shell systems discussed.

Thermoresponsive Polymer	Core	Polymerization Type	Transition Temperature [°C]	Theranostic Agent	Ref.
PNIPAm	AuNP	RAFT	32	Internalization	[84]
P(NIPAm- <i>c</i> -Am)	AuNP	FRP	37	Targeting	[85]
P(NIPAm- <i>c</i> -AAm)	AuNP	ATRP	51	ds-DNA/Dox	[86]
P(EG- <i>b</i> -CL- <i>b</i> -LA)	AuNR	ROP	55 ^{a)}	Dox	[87]
PNIPAm P(NIPAm- <i>c</i> -AA)	IOMNP	FRP	26–47	Dox	[88]
P(NIPAm- <i>c</i> -AAm)					
P(NIPAm- <i>c</i> -AAm- <i>c</i> -VP)					
PDMAEMA	IOMNP	ATRP	28–80	pDNA	[89]
POEOMA- <i>b</i> -PMMA	USIONP	ATRP	70	MRI	[90]
P(EO- <i>c</i> -PO)- <i>b</i> -PLL	LSMO	ROP	16–35	Dox	[93]
P(NIPAm- <i>c</i> -MAA)	NaYF ₄ @SiO ₂	FRP	35–37/50–65	Dox	[94]

^{a)}Crystalline transition.

core-shell systems were also used to trigger the internalization into cells upon heating over its LCST (37 °C). AuNPs were not only grafted with P(NIPAm-*c*-Am), but also with biotin which was exposed at the surface when the thermoresponsive polymer became hydrophobic at 40 °C, thereby engaging on avidin recognition. In vitro cell experiments showed cellular uptakes 17–30 times higher for the folate-SH grafted AuNPs on the folate receptor overexpressing cancer cell line KB.^[85] The same concept was applied to regulate DNA interactions in DNA-encoded drug delivery systems as shown in Figure 9. AuNPs, grafted with the thermoresponsive polymer P(NIPAm-*c*-AAm) and different double-stranded oligonucleotides (ds-DNA) (*p*CC'-Au), showed high Dox loading capacity due to Dox

intercalation between the DNA strands. Release kinetics of Dox at different temperatures showed faster drug release at temperatures higher than the LCST (51 °C). In this way, the approach improved the cytotoxicity of the encoded nanocarrier against neuroblastoma (SK-N-SH) cells.^[86]

AuNRs with a designed shell based on poly(ethylene glycol)-*b*-poly(ϵ -caprolactone) (PEG-PCL-LA) showed capabilities of remotely triggered drug release and a subsequent inhibition of drug sensitive and multidrug-resistance in cancer cells. Instead of the hydrophobic-hydrophilic transition temperature as discussed above, the authors took advantage of the phase transition of PCL regime (crystalline-soluble) here. Encapsulated Dox in crystalline PCL was released, when the temperature induced from

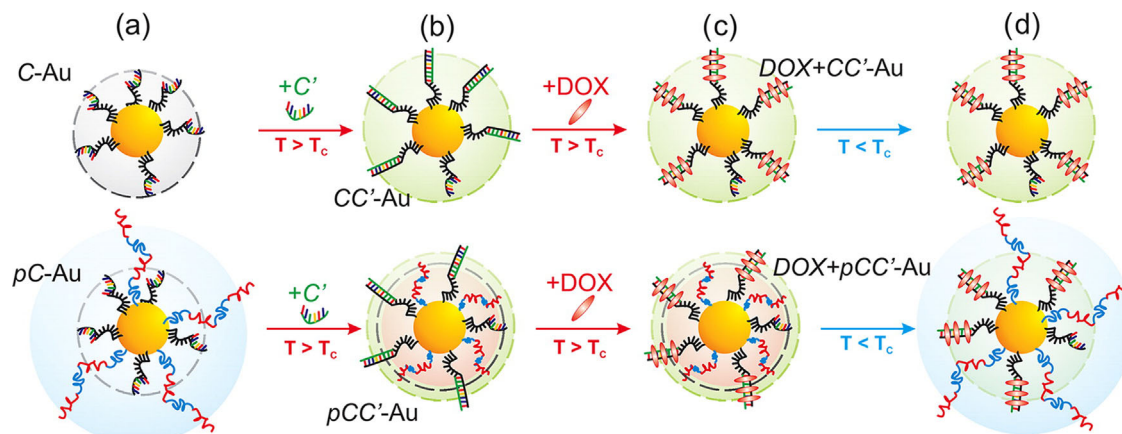


Figure 9. Preparation of the CC'-Au (top) and pCC'-Au (bottom) encoded nanocarriers from (a) ssDNA and (b) dsDNA moieties, to (c) DOX loading, and (d) the final nanocarrier before drug release at $T=37$ and 53°C . Reproduced with permission.^[86] Copyright 2013, American Chemical Society.

the phototransducer (AuNRs) reached the PCL melting point (55 °C), giving good results in the cytotoxicity tests.^[87]

Other kinds of hard nanoparticles that are also widely combined with thermoresponsive polymers to form biomedical nanodevices are the iron oxide magnetic nanoparticles (IOMNPs). Pellegrino et al. reported a design based on multiple iron oxide supermagnetic nanoparticles (nanobeads) core and different polymers based on NIPAm or *N*-isopropylmethylacrylamide (NIPMAM), as the thermosensitive shell.^[88] The LCST could be adjusted between 26 and 47 °C by copolymerization with monomers like acrylamide (AAm), allylamine, and/or *N*-vinyl-2-pyrrolidone (VP). A microfluidic platform was used to investigate the behavior of the magnetic nanostructures in the capillaries of the circulatory system. The utility of these systems for localized drug delivery triggered by a thermal and magnetic activation was demonstrated. The results revealed the absence of cargo leakage and a decrease in magnetic activity at temperatures below the LCST. Notwithstanding, heating over the transition point caused the release of Dox and the aggregation of the nanobeads into magnetic active clusters. Magnetic nanoparticles have also been tailored with pH dependant thermoresponsive polymers like PDMAEMA. PDMAEMA forms polyelectrolyte complexes with plasmid DNA (pDNA) making IOMNP@PDMAEMA, which also has a high transfection capability and low in vitro cytotoxicity, which makes it a good candidate for non-viral gene delivery. Novel magnetic isolation of animal cells without using specific ligands or receptors was achieved with this system. Polyplexes of IOMNP@PDMAEMA and pDNA, which had been transfected into the cells, were isolated and identified with the help of only a magnet.^[89] Recently, ultrasmall superparamagnetic iron oxide nanoparticles (USIONPs) were employed in a core-shell fashion with the block copolymer P(OEOMA-*b*-MAA) for in vivo magnetic resonance imaging (MRI). pH depen-

dant LCST was observed for this particular system with values in the range of 55–70 °C. Above these temperatures aggregation of the system was observed.^[90]

A great deal of attention has been recently given to lanthanum strontium manganese oxide (LSMO) magnetic nanoparticles because of their capability to produce heating energy due to hysteresis lost upon application of an alternating magnetic field (AMF).^[91,92] This property allows the use of LSMO as thermal transducers in nanomedicine. As an example, LSMO nanoparticles were coated with block thermoresponsive copolymers PEO-*b*-PLL and P(EO-*c*-PO)-*b*-PLL giving transition temperatures around 35 °C. Dox loading and release experiments at 25 and 50 °C elucidated a higher loading efficiency and loading content at 25 °C. The release increased from 10 to almost 50% upon an increase on temperature and, more interestingly, from 5 till 20% when the particles were under an alternating magnetic field.^[93]

Lin and Cheng utilized up-conversion luminescent microspheres of NaYF₄:Yb³⁺/Er³⁺ coated with a P(NIPAm-*c*-MAA) shell. The LCST of the nanoparticles constructed in this fashion was found to be pH dependant, 35–37 °C at pH = 5 and 50–65 °C when the pH was set at 7.4. When tested as a Dox nanocarrier, the particles performed a specific release at physiological temperature and slightly acidic pH in the cytotoxicity assays with SKOV3 ovarian cancer cells. In addition, these nanocarriers could also be used as luminescent tests for in vivo imaging.^[94]

3.4. Polymer Based Nanogels

Thermosensitive polymers based hydrogels and their biomedical applications have been intensively investigated in recent years (Table 5).^[95] If the hydrogel synthesis is performed within confined volume reaction vessels as nanodroplets in miniemulsions, nano-imprinting, etc.,

Table 5. Summary of the discussed thermoresponsive nanogels.

Thermoresponsive Polymer	Cross-linker	Polymerization Type	Transition Temperature [°C]	Theranostic Agent	Ref.
PNIPAm	2,2-dimethacryloxy-1-ethoxypropane	RAFT	32.0	siRNA	[98]
PMeODEGMA					
PNIPAm	Ac-dPG	FRP	32.5–34.6	Rhodamine B	[99]
PNIPAm	Ac-dPG	FRP	35.0	BSA, Asparaginase	[100]
P(NIPAm- <i>c</i> -DMAEMA)	Ac-dPG	FRP	40.9	Dox/MTX	[101]
POEGMA	Ac-dPG	FRP	25–45	Rhodamine B	[102]
P(GME- <i>c</i> -EGE)	Oct-dPG	ROP	30–50	Dox	[103]
P(NIPAm- <i>c</i> -AA)	AuNR@SiO ₂	FRP	39	Dox	[104]
PAA-hp-DNA	Au-AgNR@SiO ₂	ATRP/ROP	35–41	Dox	[105]
PVA	Bi ₂ O ₃ QD	FRP	37–40	QD/TMZ	[106]

particles with nanometric sizes are obtained.^[96,97] These kinds of systems, so-called nanogels, have been very interesting for the biomedical research community because they have similar dimensions to biomacromolecules like proteins, viruses, receptor clustering in cells, etc. which widens the range of applications for polymeric materials. One of the latest examples reported was synthesized by RAFT using poly(2-glucoamidoethylmethacrylamide) P(GAEMA)₆₃ as a macro-chain transfer agent, NIPAm, 2-aminoethylmethacrylamide (AEMA), methoxydiethylene glycol methacrylate (MeODGM) as monomers, and 2,2-dimethacryloxy-1-ethoxypropane as the cross-linker. These tailor-made thermoresponsive cationic glyconanogels were constructed and efficiently proved as nano-carriers for siRNA delivery.^[98]

Calderón et al. applied the already mentioned desirable properties of dPG to thermoresponsive nanosystems. dPGs functionalized with acrylic groups (Ac-dPG) have been shown to be useful as cross-linkers for nanogel synthesis. In a preliminary study of the nanogels based on PNIPAm and Ac-dPG synthesized by precipitation polymerization, it was shown that the nanogel size and the LCST (32.5 to 34.6 °C) could be tuned by changing the dPG feed ratio. Internalization studies performed in human hematopoietic U-937 cells with rhodamin B labelled nanogels showed good

internalization and low cytotoxicity (Figure 10).^[99] The same nanogels were used for targeted dermal protein delivery. Release of bovine serum albumin (BSA) and asparaginase in pig skin occurred upon temperature triggering specifically into the viable epidermis of barrier-deficient skin without loss of protein integrity and bioactivity.^[100] An improvement of this concept was recently published by the same group by copolymerizing PNIPAm with DMAEMA and introducing a pH-responsive modality to the nanogels. The LCST of the nanogels increased to the more useful value of 40.9 °C for thermally induced drug delivery applications. The positively charged nanogels presented a higher loading capacity and efficiency of Dox (approximately 2 folds) but no changes were observed for methotrexate (MTX). Higher values were obtained in the release profile of the charged nanogels in comparison to the NIPAm ones, and the release kinetic was faster over the LCST of the system.^[101] In the same way, OEGMA was also explored in the construction of nanogels that can penetrate through human skin upon a thermal trigger.^[102]

Calderón et al. employed dPG as a macro-cross-linker and linear poly(glycidyl methyl ether-co-ethyl glycidyl ether) [P(GME-*c*-EGE)] as a thermo-responsive polymer to synthesize nanogels via a novel synthetic method, so-called

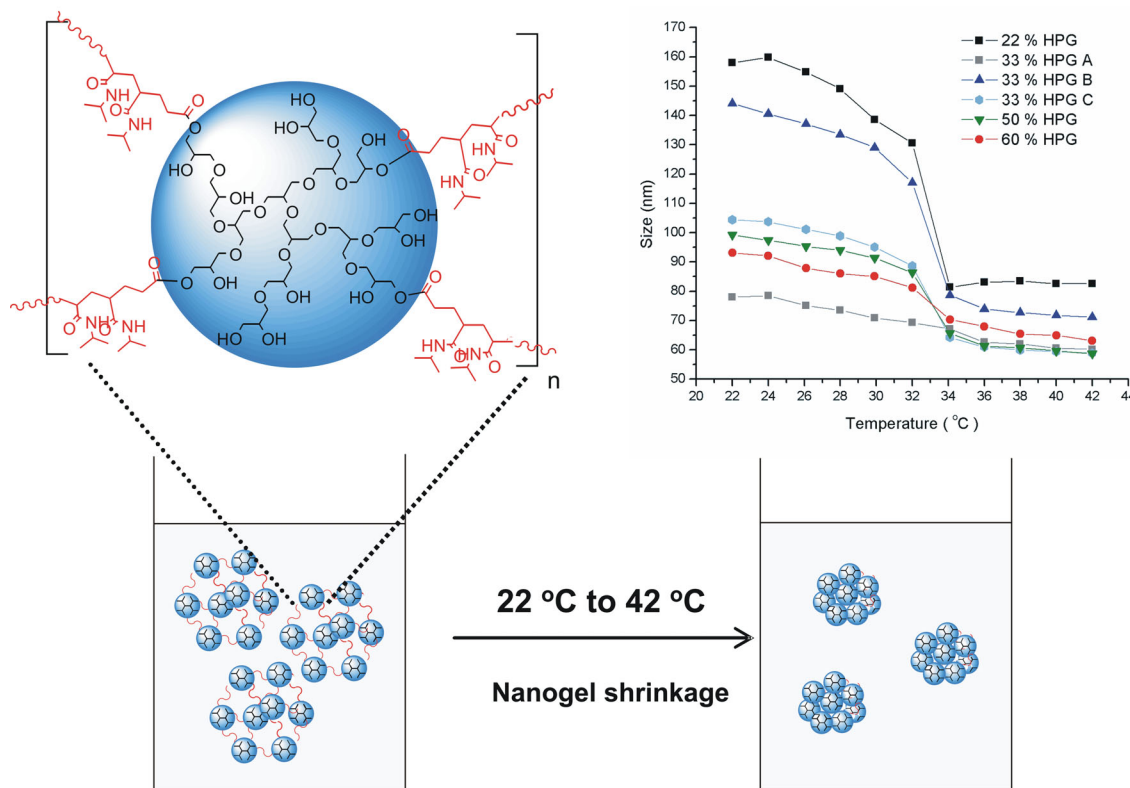


Figure 10. Schematic representation of the synthesis of nanogels by precipitation polymerization of PNIPAm and Ac-dPG. Reproduced with permission^[99] Copyright 2011, Royal Society of Chemistry.

thermo-nanoprecipitation (TNP). The strain-promoted azide alkyne cycloaddition of the prefunctionalized polymers was employed to form the cross-linking points, via a methodology that did not require an input of energy, elevated temperature, or the presence of stabilizer. Nanogels proved to have tunable transition temperatures in the range of 30–50 °C depending on the ratio of copolymer employed. Internalization studies were engaged with Cy5 labeled nanogels in A549 tumor cells which indicated their potential as drug carriers. To demonstrate the encapsulation ability of the tNG, Dox was chosen as an anti-cancer drug model and a 52.40 wt% was achieved by encapsulation in the nanoparticle synthesis.^[103]

3.5. AuNR Based Nanogels

The advantages of hard nanoparticles as photothermal transducers were also exploited in nanogel-like architectures as summarized in Table 5. Silica-coated AuNRs were entrapped in PNIPAM nanogel by making use of the seed precipitation polymerization nanogelification technique. The obtained hybrid nanogels showed minimal cytotoxicity and high biocompatibility in cell experiments as well as pH and thermo dependency ($LCST = 39^\circ\text{C}$ at pH 7.4). Dox was loaded into the nanocarriers through electrostatic interactions up to 24% in loading content, and the release was examined in mice models upon NIR laser activation. The NIR laser irradiation not only triggered the drug release, but also induced actively targeted cancer cells without using active target ligands. NIR radiation enhanced the nanocomposite's accumulation in tumor postsystematic administration with almost a completely inhibited tumor growth and lung metastasis (Figure 11). This work

represents one of the smartest NIR guided drug delivery systems up to date.^[104]

Gold-silver nanorods (Ag-AuNRs) have been used as phototransducers in PAA based nanogels, cross-linked by complementary DNA strands. Nanogels were functionalized with DNA aptamers for specific recognition of tumor cells. Dox was loaded into DNA aptamers which responded upon NIR radiation releasing the drug. Studies in CCRF-CEM cells and Ramos cell line as the control demonstrated low cytotoxicity of the nanogels as well as high specificity for tumor cells after NIR irradiation.^[105]

Temperature-responsive hybrid nanogels formed by Bi_2O_3 QDs and poly(vinyl alcohol) (PVA) were reported by Wu and Zhou. QDs were shown to cooperatively work with the gel networks of PVA to enable a volume phase transition of the nanogels in the range of 37 to 40 °C. These nanogels were loaded with temozolomide (TMZ) as model drug that was effectively released upon thermal triggering. In addition, the QDs fluorescent properties were recovered. These systems were not only designed as theranostic devices acting as drug nanocarriers or imaging probes, but also as nanothermometers for in vivo reporting of the temperature dependant fluorescence intensity.^[106]

4. Conclusion

In summary, the increasing application of thermoresponsive materials as smart nanocarriers proves that the field of nanomedicine is constantly evolving towards more sophisticated, controlled, and well defined systems. This evolution is augmented nowadays by the multitude of possibilities that novel synthetic building blocks offer.

Careful and rational selection of building blocks can be realized by paying attention to specific drug requirements, targeting to the site of action, and environmentally triggered theranostic application. This feature article highlights examples of the great arsenal on hand for polymer chemists who develop thermoresponsive nanodevices.

Soft dendritic polymers and hard nanoparticles contribute to the construction of systems with interesting properties for theranostics purposes. Different architectures were studied that increased in order of complexity from the ones formed with block copolymers, non cross-linked structures like micelles or vesicles, to core-shells or nanogel like systems that allow the use of hybrid organic/inorganic materials with precise control of the structure. However, only the less

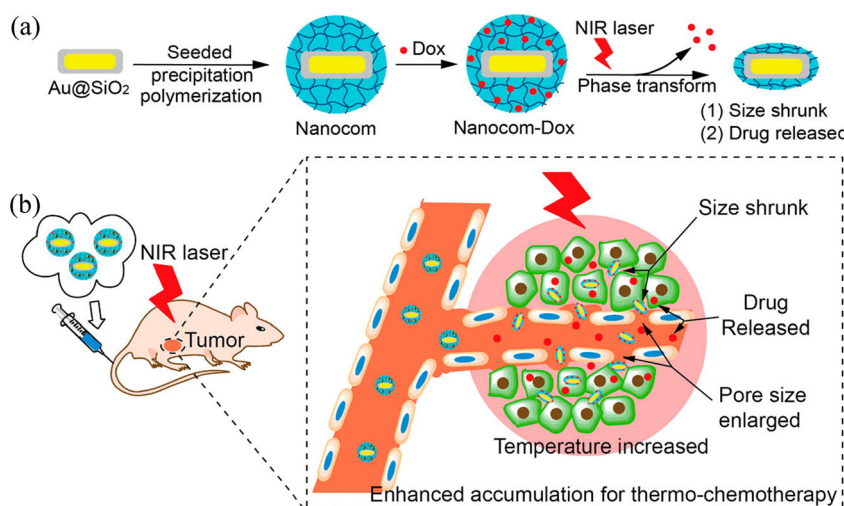


Figure 11. (A) Hybrid nanogel formulation process and (B) NIR laser induced targeted thermo-chemotherapy using the nanogel. Reproduced with permission.^[104] Copyright 2014, American Chemical Society.

complex systems are in an advanced clinical phase.^[107] For example pluronic micelles loaded with the anti-cancer drug Dox (Dox; SP1049C) have reached Phase I and II clinical trials. The SP1049C formulation showed promising results including slower clearance than with conventional Dox, as well as evidence for anti-tumor activity in some patients with advanced resistant solid tumors.^[108,109] These results support the great potential of thermoresponsive nanodevices for anti-cancer treatment in particular, and for medicine in general. Still a big effort, however, has to be done before most of the examples here described can make their way from the bench to clinics.

Acknowledgements: We gratefully acknowledge financial support from the Bundesministerium für Bildung und Forschung (BMBF) through the NanoMatFutur award (13N12561), and the Helmholtz Virtual Institute, Multifunctional Biomaterials for Medicine and the Freie Universität Focus Area Nanoscale. The authors acknowledge support from Deutsche Forschungsgemeinschaft (DFG)/German Research Foundation via SFB1112, Project A04. Dr. Julian Bergueiro acknowledges financial support from Dahlem Research Center through the Dahlem International Network Postdocs program. We gratefully acknowledge Dr. Pamela Winchester for proofreading the manuscript.

Received: August 7, 2014; Revised: September 11, 2014; Published online: October 16, 2014; DOI: 10.1002/mabi.201400362

Keywords: drug delivery; nanocarriers; nanomedicine; theranostics; thermoresponsive

- [1] E. K.-H. Chow, D. Ho, *Sci. Translat. Med.* **2013**, *5*, 216rv4.
- [2] H. Maedaa, J. Wu, T. Sawaa, Y. Matsumurab, K. Horic, *J. Controlled Release* **2000**, *65*, 271.
- [3] J. Khandare, M. Calderon, N. M. Dagia, R. Haag, *Chem. Soc. Rev.* **2012**, *41*, 2824.
- [4] R. Haag, F. Kratz, *Angew. Chem. Int. Ed.* **2006**, *45*, 1198.
- [5] T. Krasia-Christoforou, T. K. Georgiou, *J. Mater. Chem. B* **2013**, *1*, 3002.
- [6] T. Lammers, S. Aime, W. E. Hennink, G. Storm, F. Kiessling, *Acc. Chem. Res.* **2011**, *44*, 1029.
- [7] S. S. Kelkar, T. M. Reineke, *Bioconjug. Chem.* **2011**, *22*, 1879.
- [8] S. Reichert, M. Calderon, K. Licha, R. Haag, "Multivalent Dendritic Architectures in Theranostics". in: *Multifunctional Nanoparticles for Medical Applications: Imaging, Targetting and Drug Delivery*, Springer, Berlin/New York **2012**, p. 315.
- [9] M. Calderon, M. A. Quadir, M. Strumia, R. Haag, *Biochimie* **2010**, *92*, 1242.
- [10] M. A. Ward, T. K. Georgiou, *Polymers* **2011**, *3*, 1215.
- [11] N. T. Southall, K. A. Dill, A. D. J. Hayment, *J. Phys. Chem. B* **2002**, *106*, 521.
- [12] B. Zhang, H. Tang, P. Wu, *Macromolecules* **2014**, *47*, 4728.
- [13] L. Klouda, A. G. Mikos, *Eur. J. Pharm. Biopharm.* **2008**, *68*, 34.
- [14] J.-F. Lutz, *J. Polym. Sci., Part A* **2008**, *46*, 3459.
- [15] Z. Zarafshani, T. Obata, J.-F. Lutz, *Biomacromolecules* **2010**, *11*, 2130.
- [16] J. F. Lutz, A. Hoth, *Macromolecules* **2006**, *39*, 893.
- [17] F. A. Plamper, M. Ruppel, A. Schmalz, O. Borisov, M. Ballauff, A. H. E. Mueller, *Macromolecules* **2007**, *40*, 8361.
- [18] A. Schmalz, M. Hanisch, H. Schmalz, A. H. E. Müller, *Polymer* **2010**, *51*, 1213.
- [19] J. K. Lam, Y. Ma, S. P. Armes, A. L. Lewis, T. Baldwin, S. Stolnik, *J. Controlled Release* **2004**, *100*, 293.
- [20] H. Viola, A. Laukkanen, L. Valtola, H. Tenhu, J. Hirvonen, *Biomaterials* **2005**, *26*, 3055.
- [21] H. Viola, A. Laukkanen, H. Tenhu, J. Hirvonen, *J. Pharm. Sci.* **2008**, *97*, 4783.
- [22] A. C. Lau, C. Wu, *Macromolecules* **1999**, *32*, 581.
- [23] F. Meeussen, E. Niesa, H. Berghmans, S. Verbrugghe, E. Goethals, F. D. Prez, *Polymer* **2000**, *41*, 8597.
- [24] J. Hao, J. Servello, P. Sista, M. C. Biewer, M. C. Stefan, *J. Mater. Chem.* **2011**, *21*, 10623.
- [25] N. Saha, *J. Biomat. Nanobiotech.* **2011**, *2*, 85.
- [26] D. J. Phillips, M. I. Gibson, *Chem. Commun.* **2012**, *48*, 1054.
- [27] K. Rahimian-Bajgiran, N. Chan, Q. Zhang, S. M. Noh, H. I. Lee, J. K. Oh, *Chem. Commun.* **2013**, *49*, 807.
- [28] R. París, M. Liras, I. Quijada-Garrido, *Macromol. Chem. Phys.* **2011**, *212*, 1859.
- [29] N. S. Leong, M. Hasan, D. J. Phillips, Y. Saaka, R. K. O'Reilly, M. I. Gibson, *Polym. Chem.* **2012**, *3*, 794.
- [30] W. A. Braunecker, K. Matyjaszewski, *Prog. Polym. Sci.* **2007**, *32*, 93.
- [31] C. Boyer, V. Bulmus, T. P. Davis, V. Ladrinal, J. Liu, S. B. Perrier, *Chem. Rew.* **2009**, *109*, 5402.
- [32] D. J. Siegwart, J. K. Oh, K. Matyjaszewski, *Prog. Polym. Sci.* **2012**, *37*, 18.
- [33] O. Nuyken, S. Pask, *Polymers* **2013**, *5*, 361.
- [34] A. Chilkoti, M. R. Dreher, D. E. Meyer, *Adv. Drug Delivery Rev.* **2002**, *54*, 1093.
- [35] W. Kim, E. L. Chaikof, *Adv. Drug Delivery Rev.* **2010**, *62*, 1468.
- [36] J. R. McDaniel, D. J. Callahan, A. Chilkoti, *Adv. Drug Delivery Rev.* **2010**, *62*, 1456.
- [37] D. L. Nettles, A. Chilkoti, L. A. Setton, *Adv. Drug Delivery Rev.* **2010**, *62*, 1479.
- [38] J. L. Frandsen, H. Ghandehari, *Chem. Soc. Rev.* **2012**, *41*, 2696.
- [39] C. Z. Wei, C. L. Hou, Q. S. Gu, L. X. Jiang, B. Zhu, A. L. Sheng, *Biomaterials* **2009**, *30*, 5534.
- [40] K. Zhang, Y. Qian, H. Wang, L. Fan, C. Huang, A. Yin, X. Mo, J. *Biomed. Mater. Res. A* **2010**, *95*, 870.
- [41] J. M. Dang, D. D. Sun, Y. Shin-Ya, A. N. Sieber, J. P. Kostuk, K. W. Leong, *Biomaterials* **2006**, *27*, 406.
- [42] A. T. Jonstrup, J. Fredsoe, A. H. Andersen, *Sensors* **2013**, *13*, 5937.
- [43] M. Kaur, M. Makrigiorgos, *Nucleic Acids Res.* **2003**, *31*, 266.
- [44] H. Chung, Y.-K. Kim, D. Shin, S.-R. Ryoo, B.-H. Hong, D.-H. Min, *Acc. Chem. Res.* **2013**, *46*, 2211.
- [45] N. Fomina, C. L. McFearin, M. Sermsakdi, J. M. Morachis, A. Almutairi, *Macromolecules* **2011**, *44*, 8590.
- [46] R. Weissleder, *Nat. Biotech.* **2001**, *19*, 316.
- [47] V. Ntziachristos, A. G. Yodh, M. Schnall, B. Chance, *Proc. Natl. Acad. Sci.* **2000**, *97*, 2767.
- [48] A. Kumar, B. Mazinder Boruah, X.-J. Liang, *J. Nanomater.* **2011**, DOI 10.1155/2011/747196.
- [49] S. Laurent, D. Forge, M. Port, A. Roch, C. Robic, L. V. Elst, R. N. Muller, *Chem. Rew.* **2008**, *108*, 2064.
- [50] H. S. Huang, J. F. Hainfeld, *Int. J. Nanomedicine* **2013**, *8*, 2521.
- [51] A. J. Giustini, A. A. Petryk, S. M. Cassim, J. A. Tate, I. Baker, P. J. Hoopes, *Nano Life* **2010**, DOI 10.1142/S1793984410000067.
- [52] H. Yim, S. Seo, K. Na, *J. Nanomater.* **2011**, DOI 10.1155/2011/747196.

- [53] M. N. Rhyner, A. M. Smith, X. Gao, H. Mao, L. Yang, S. Nie, *Nanomedicine* **2006**, *1*, 209.
- [54] M.-C. Jones, J.-C. Leroux, *Eur. J. Pharm. Biopharm.* **1999**, *48*, 101.
- [55] G. Riess, *Prog. Polym. Sci.* **2003**, *28*, 1107.
- [56] J. Lao, J. Madani, T. Puertolas, M. Alvarez, A. Hernandez, R. Pazo-Cid, A. Artal, A. A. Torres, *J. Drug Delivery* **2013**, DOI 10.1155/2013/456409.
- [57] W. Xu, P. Ling, T. Zhang, *J. Drug Deliv.* **2013**, DOI 10.1155/2013/340315.
- [58] Y. Hiruta, M. Shimamura, M. Matsuura, Y. Maekawa, T. Funatsu, Y. Suzuki, E. Ayano, T. Okano, H. Kanazawa, *ACS Macro Lett.* **2014**, *3*, 281.
- [59] J. Akimoto, M. Nakayama, K. Sakai, T. Okano, *Mol. Pharmaceutics* **2010**, *7*, 926.
- [60] W. Li, J. Li, J. Gao, B. Li, Y. Xia, Y. Meng, Y. Yu, H. Chen, J. Dai, H. Wang, Y. Guo, *Biomaterials* **2011**, *32*, 3832.
- [61] R. P. Johnson, Y.-I. Jeong, J. V. John, C.-W. Chung, D. H. Kang, M. Selvaraj, H. Suh, I. Kim, *Biomacromolecules* **2013**, *14*, 1434.
- [62] X. Wan, T. Liu, S. Liu, *Biomacromolecules* **2011**, *12*, 1146.
- [63] Y. Li, Y. Qian, T. Liu, G. Zhang, S. Liu, *Biomacromolecules* **2012**, *13*, 3877.
- [64] Y. Shao, Y.-G. Jia, C. Shi, J. Luo, X. X. Zhu, *Biomacromolecules* **2014**, *15*, 1837.
- [65] E. A. Rainbolt, K. E. Washington, M. C. Biewer, M. C. Stefan, *J. Mater. Chem. B* **2013**, *1*, 6532.
- [66] K. Yang, T. Gao, Z. Bao, J. Su, X. Chen, *J. Mater. Chem. B* **2013**, *1*, 6442.
- [67] A. J. Simnick, M. Amiram, W. Liu, G. Hanna, M. W. Dewhurst, C. D. Kontos, A. Chilkoti, *J. Controlled Release* **2011**, *155*, 144.
- [68] A. J. Simnick, C. A. Valencia, R. Liu, A. Chilkoti, *ACS Nano* **2010**, *4*, 2217.
- [69] P. V. Pawar, S. V. Gohil, J. P. Jain, N. Kumar, *Polym. Chem.* **2013**, *4*, 3160.
- [70] J. S. Lee, W. Zhou, F. Meng, D. Zhang, C. Otto, J. Feijen, *J. Controlled Release* **2010**, *146*, 400.
- [71] Z.-Y. Qiao, R. Ji, X.-N. Huang, F.-S. Du, R. Zhang, D.-H. Liang, Z.-C. Li, *Biomacromolecules* **2013**, *14*, 1555.
- [72] X. Y. Xiong, Y. P. Li, Z. L. Li, C. L. Zhou, K. C. Tam, Z. Y. Liu, G. X. Xie, *J. Controlled Release* **2007**, *120*, 11.
- [73] W. Zhang, K. Gilstrap, L. Wu, R. Bahadur K. C., M. A. Moss, Q. Wang, X. Lu, X. He, *ACS Nano* **2010**, *4*, 6747.
- [74] S. Sanyal, H.-G. Huang, K. Rege, L. L. Dai, *J. Nanomed. Nanotechnol.* **2011**, *2*, 1000126.
- [75] Y. Zhao, X. Fan, D. Liu, Z. Wang, *Int. J. Pharm.* **2011**, *409*, 229.
- [76] S. J. T. Rezaei, M. R. Nabid, H. Niknejad, A. A. Entezami, *Polymer* **2012**, *53*, 3485.
- [77] H. Wan, Y. Zhang, Z. Liu, G. Xu, G. Huang, Y. Ji, Z. Xiong, Q. Zhang, J. Dong, W. Zhang, H. Zou, *Nanoscale* **2014**, *6*, 8743.
- [78] J. Yin, J. Hu, G. Zhang, S. Liu, *Langmuir* **2014**, *30*, 2551.
- [79] N. S. Rejinold, K. P. Chennazhi, S. V. Nair, H. Tamura, R. Jayakumar, *Carbohydr. Polym.* **2011**, *83*, 776.
- [80] C. Kojima, K. Irie, *Biopolymers* **2013**, *100*, 714.
- [81] E. Boisselier, D. Astruc, *Chem. Soc. Rev.* **2009**, *38*, 1759.
- [82] M.-C. Daniel, D. Astruc, *Chem. Rev.* **2004**, *104*, 293.
- [83] NŽ. Knežević, E. Ruiz-Hernández, W. E. Hennink, M. Vallet-Regí, *RSC Adv.* **2013**, *3*, 9584.
- [84] M. Liang, I. C. Lin, M. R. Whittaker, R. F. Minchin, M. J. Monteiro, I. Toth, *ACS Nano* **2010**, *4*, 403.
- [85] F. Mastrotto, P. Caliceti, V. Amendola, S. Bersani, J. P. Magnusson, M. Meneghetti, G. Mantovani, C. Alexander, S. Salmaso, *Chem. Commun.* **2011**, *47*, 9846.
- [86] K. L. Hamner, C. M. Alexander, K. Coopersmith, D. Reishofer, C. Provenza, M. M. Maye, *ACS Nano* **2013**, *7*, 7011.
- [87] Y. Zhong, C. Wang, L. Cheng, F. Meng, Z. Zhong, Z. Liu, *Biomacromolecules* **2013**, *14*, 2411.
- [88] M. Pernia Leal, A. Torti, A. Riedinger, R. La Fleur, D. Petti, R. Cingolani, R. Bertacco, T. Pellegrino, *ACS Nano* **2012**, *6*, 10535.
- [89] A. P. Majewski, A. Schallol, V. Jérôme, R. Freitag, A. H. E. Müller, H. Schmalz, *Biomacromolecules* **2012**, *13*, 857.
- [90] N. Chan, M. Laprise-Pelletier, P. Chevallier, A. Bianchi, M.-A. Fortin, J. K. J. Oh, *Biomacromolecules* **2014**, *15*, 2146.
- [91] S. Laurent, S. Dutz, U. O. Hafeli, M. Mahmoudi, *Adv. Colloid. Interface Sci.* **2011**, *166*, 8.
- [92] A. Figueroa, R. Di Corato, L. Manna, T. Pellegrino, *Pharmacol. Res.* **2010**, *62*, 126.
- [93] S. Louguet, B. Rousseau, R. Epherre, N. Guidolin, G. Goglio, S. Mornet, E. Duguet, S. Lecommandoux, C. Schatz, *Polym. Chem.* **2012**, *3*, 1408.
- [94] Y. Dai, Pa. Ma, Z. Cheng, X. Kang, X. Zhang, Z. Hou, C. Li, D. Yang, X. Zhai, J. Lin, *ACS Nano* **2012**, *6*, 3327.
- [95] Z. Y. Qian, S. Z. Fu, S. S. Feng, *Nanomedicine* **2013**, *8*, 161.
- [96] M. Asadian, A. Souza, J. Cuggio, D. Steinhilber, M. Calderon, *Curr. Med. Chem.* **2012**, *19*, 5029.
- [97] A. L. Sisson, R. Haag, *Soft Matter* **2010**, *6*, 4968.
- [98] M. Ahmed, P. Wattanaarsakit, R. Narain, *Polym. Chem.* **2013**, *4*, 3829.
- [99] J. C. Cuggino, C. I. Alvarez, I. M. C. Strumia, P. Welker, K. Licha, D. Steinhilber, R.-C. Mutihac, M. Calderón, *Soft Matter* **2011**, *7*, 11259.
- [100] M. Molina, M. Witting, W. Friess, S. Küchler, M. Calderon, presented at 41st Annual Meeting and Exposition Controlled Released Society, Chicago, July **2014**.
- [101] M. A. Molina, M. Giulbudagian, M. Calderón, *Macromol. Chem. Phys.* **2014**, DOI: 10.1002/macp.201400286.
- [102] M. Asadian-Birjand, F. Rancan, J. C. Cuggino, K. Achazi, R. C. Mutihac, J. Dernedde, A. Vogt, M. Calderón, presented at 41st Annual Meeting and Exposition Controlled Released Society, Chicago, July **2014**.
- [103] M. Giulbudagian, M. Asadian-Birjand, D. Steinhilber, K. Achazi, M. A. Molina, M. Calderón, *Polymer Chem.* **2014**, DOI 10.1039/C4PY01186D.
- [104] Z. Zhang, J. Wang, X. Nie, T. Wen, Y. Ji, X. Wu, Y. Zhao, C. Chen, *J. Am. Chem. Soc.* **2014**, *136*, 7317.
- [105] H. Kang, A. C. Trondoli, G. Zhu, Y. Chen, Y.-J. Chang, H. Liu, X.-F. Huang, X. Zhang, W. Tan, *ACS Nano* **2011**, *5*, 5094.
- [106] H. Zhu, Y. Li, R. Qiu, L. Shi, W. Wu, S. Zhou, *Biomaterials* **2012**, *33*, 3058.
- [107] C. Oerlemans, W. Bult, M. Bos, G. Storm, J. F. Nijsen, W. E. Hennink, *Pharm. Res.* **2010**, *27*, 2569.
- [108] S. Danson, D. Ferry, V. Alakhov, J. Margison, D. Kerr, D. Jowle, M. Brampton, G. Halbert, M. Ranson, *Br. J. Cancer* **2004**, *90*, 2085.
- [109] M. Talelli, W. E. Hennink, *Future Med.* **2011**, *6*, 1245.